

## Fabrication of biocomposites reinforced with natural fibers and evaluation of their physio-chemical properties

Jumiarti Andi Lolo <sup>1</sup>, Siti Nikmatin <sup>2,3</sup>, Husin Alatas <sup>2</sup>, Dedy Dwi Prastyo <sup>4</sup>, Achmad Syafiuddin <sup>5,\*</sup> 

<sup>1</sup>Physics Education, Universitas Kristen Indonesia Toraja, 91811 Tana Toraja, South Sulawesi, Indonesia

<sup>2</sup>Department of Physics, Faculty of Mathematics and Natural Sciences, IPB University (Bogor Agricultural University), 16680 Bogor, West Java, Indonesia

<sup>3</sup>Surfactant and Bioenergy Research Center (SBRC), IPB University (Bogor Agricultural University), IPB Darmaga Campus, 16680 Bogor, Indonesia

<sup>4</sup>Department of Statistics, Faculty of Science and Data Analytics, Institut Teknologi Sepuluh Nopember, 60111 Surabaya, East Java, Indonesia

<sup>5</sup>Department of Water and Environmental Engineering, Faculty of Engineering, Universiti Teknologi Malaysia, 81310 UTM Johor Bahru, Johor, Malaysia

\* corresponding author e-mail address: [ac.syafi@gmail.com](mailto:ac.syafi@gmail.com) | Scopus ID [56682128000](https://orcid.org/0000-0002-5668-2128)

### ABSTRACT

The present study aims to fabricate and evaluate the physio-chemical features of biocomposites filled with natural resources. Kenaf was used as a natural resource model and prepared by mechanical milling and sieving to obtain short fiber form. Virgin and recycled acrylonitrile butadiene styrene (ABS) were used as biocomposite matrix. Granular biocomposite was fabricated using the single screw extruder with the natural filler content variations ranging from 10 to 15%. Chemical composition, density, and dimension of the fabricated fillers were examined. Melt flow index, surface free energy, and functional group characteristics of the presently fabricated biocomposites were also evaluated. Analysis of the chemical composition, density, and dimension confirmed the physio-chemical characteristics of the fabricated fillers. The biocomposites density and melt flow index were slightly enhanced with the rise of the filler content. Contact angle, dispersive component, polar component, and surface free energy of biocomposites varied depending on the filler content and ABS type. Fourier transforms infrared spectroscopy analysis confirmed the functional groups of the biocomposites. In general, this work has successfully fabricated and evaluated the physio-chemical characteristics of composites filled with kenaf. The produced biocomposites can be a good strategy to produce high performance polymer biocomposites for future applications.

**Keywords:** *Biocomposites; acrylonitrile butadiene styrene; surface free energy.*

### 1. INTRODUCTION

Development of biomaterials is rapidly expanding and has the potential prospect for the future [1-6]. This is because natural resources as basic reinforcements are abundantly available [7]. In addition, there are evidence in scientific literature that the performance of composites filled with natural resources is comparable with those filled with synthetic materials [8,9]. In addition, the use of natural filler has several advantages such as low density, low cost, renewable, and recyclable [10]. *Hibiscus cannabinus* is a natural resource that is widely explored as a filler for fabricating biocomposites because of its high cellulose content.

A combination of natural fibers and polymers provides a positive impact on the environments such as reducing the release of carbon gas and environmental impact of non-biodegradable material. Acrylonitrile butadiene styrene (ABS) is a type of polymer that is commonly explored as a matrix to produce biocomposites [11]. ABS becomes popular since it has been proven to have superior mechanical properties, chemical resistance, easily processed, and recyclable [12]. In general, a coupling agent is required to bind between nonpolar and polar materials such as polymers and cellulose, respectively.

Several studies have explored the novel properties of biocomposites for diverse field applications [13-16]. For instance, the chitosan-smectite biocomposite fabricated using the intercalation of protonated chitosan molecules into the interlayer space of smectite through cation exchange mechanism was proposed for the novel potentiometric monohydrogen phosphate-selective sensor [17]. Their study verified that the biocomposites

exhibited good performances in terms of sensitivity, stability, response time, detection limit, and a wide linear range for monohydrogen phosphate ions detection. Alternatively, the chitosan-lysozyme biocomposites exhibited the capability as an adsorbent to remove methyl orange dye and hexavalent chromium ions by maximum adsorption capacities of 435 and 216 mg/g, respectively [18]. Moreover, the biocomposites reinforced by fibers have also been widely explored for medical applications such as tissue engineering or regenerative medicine [19].

The properties of biocomposites can be influenced by several factors such as filler characteristics, filler loading, preparation procedure, and interface properties of filler in their matrix. Fabrication of biocomposites commonly involves the role of heat and mechanical such as milling, extrusion, and injection molding. Therefore, melt flow index determination is an important aspect to characterize the ability of biocomposites to load heat. Treatment on the surface of composites such as coating can affect the adhesion properties of biocomposites. Surface free energy is a criterion that is widely used to determine adhesion properties of biocomposites. In addition, the properties of biocomposites are also highly influenced by their internal structure. Each molecule in biocomposites has a natural vibration, which depends on the type and chemical bonding. Natural vibration of molecules is an indicator for the identification of molecules present in the materials. Identification of functional group of biocomposites can be easily performed using the infrared spectrophotometers such as Fourier transform infrared spectroscopy. From the above mentioned

overview, it is possible to fabricate a few trends for the behavior of polymer matrix composites based on the nature of the polymer matrix and filler.

Aligning the aforementioned research necessity, this work was aimed to fabricate and evaluate the physico-chemical features

## 2. MATERIALS AND METHODS

### 2.1. Materials.

Kenaf having a length of 4 m was obtained from the kenaf plantation under PT Global Agrotek Nusantara, Pekanbaru, Riau, Indonesia. Virgin and recycled ABS polymers were purchased from PT MUB Jaya, Bogor, Indonesia. Additive chemicals were maleic acid (Darmstadt, Germany) used as a coupling agent and primary antioxidant (Zaozhuang, China).

### 2.2. Short fibers fabrication.

Kenaf fibers were processed by soaking dynamically in the water for two weeks and then dried under the sun. Furthermore, the fibers were cut with a uniform length of  $\pm 1$  cm and then dried in an oven (Tipe YNC-OV, YENACO, China) at 40 °C for 24 h. The dried kenaf was taken from the oven and then milled using a milling machine (Model MDY-1000, FOMAC, China). After the milling process, the sample was screened by using 20 mesh sieve and was selected as short fibers. The chemical composition of fiber was determined according to the technical association of the pulp and paper industry (TAPPI) standardization. Kenaf fiber and biocomposites densities were estimated using the Archimedes approach. Dimension of the fiber was estimated from images (Model BX51, Olympus, Japan) combined with the software olympus DP2-BSW and DP25 olympus microscope camera.

### 2.3. Preparation of biocomposites.

Granular biocomposite was fabricated by mixing kenaf short fiber as a filler, ABS polymer as a matrix, maleic acid as coupling agent, and primary antioxidant with the biocomposite composition as listed in Table 1.

Table 1. Composition of the presently fabricated biocomposites

| Sample       | Kenaf short fiber | ABS polymer | Primary antioxidant | Maleic acid |
|--------------|-------------------|-------------|---------------------|-------------|
| vABS-KSF-10% | 10 %              | 87 %        | 1%                  | 2%          |
| vABS-KSF-15% | 15 %              | 82 %        | 1%                  | 2%          |
| rABS-KSF-10% | 10 %              | 87 %        | 1%                  | 2%          |
| rABS-KSF-15% | 15 %              | 82 %        | 1%                  | 2%          |

All samples were fabricated using the single screw extrusion (Model HXSJ-125/125, Kai Xin, China). Test pieces were prepared using the molding injection machine (Model HC-250, Hwa Chin, China) In the preparation, 5 kg of granular biocomposite was put into the hopper of molding injection and then heated at a

of biocomposites filled with natural resources. Specifically, ABS and kenaf were employed as a matrix and a filler for the presently fabricated biocomposites, respectively. Outcomes from this work are highly beneficial in improving the biocomposites properties that are important for future applications.

temperature of 80 °C. Barrel of the molding injection was heated at 5 different temperatures (120 °C to 200 °C). Therefore, vABS-KSF-10%, vABS-KSF-15%, rABS-KSF-10%, and rABS-KSF-15% denote to virgin ABS with 10% of filler, virgin ABS with 15% of filler, recycled ABS with 10% of filler, and recycled ABS with 15% of filler, respectively.

### 2.4. Melt flow index investigation.

Melt flow index (MFI) is a measure of polymer melting rate expressed by the weight of polymer in gram run for 10 mins through the capillaries. Biocomposites MFI measurements were performed using the melt flow indexer (Model XNR-400D, Jinan Hensgrand Instrument, Cina) at a temperature of 220 °C.

### 2.5. Fourier transforms infrared spectroscopy analysis.

Fourier transforms infrared spectroscopy (FTIR) analysis was conducted by measuring the transmittance of materials using the FTIR equipment (ABB, model MB300, Canada) observed within the wavenumber range from 4000  $\text{cm}^{-1}$  to 400  $\text{cm}^{-1}$ . The sample was formed into pellets with potassium bromide.

### 2.6. Surface free energy determination.

Contact angle measurement was observed through the sessile droplet method using Phoenix 300 contact angle analyzer (Surface Electro Optics, Korea) and was analysed based on equation [20]:

$$\gamma_l \cos \theta = \gamma_s - \gamma_{sl} \tag{1}$$

where  $\gamma_l$  denotes the surface free energy of liquid in contact with the solid and  $\gamma_{sl}$  represents the interfacial free energy between solid and the liquid. In order to solve this equation for  $\gamma_s$ , it needs to add another equation that correlates  $\gamma_{sl}$  with  $\gamma_l$  and  $\gamma_s$ . It was proposed that the polar interaction could be computed using the same geometric mean mixing rule as for the dispersion force interaction [21]. If the contact angle of at least two liquids (polar and nonpolar), with known  $\gamma_l^d$  and  $\gamma_l^p$  parameters are measured on a solid surface,  $\gamma_s^d$  and  $\gamma_s^p$  parameters of that solid can be estimated. Hence, the following equation was used:[21]

$$\gamma_{sl} = \gamma_s + \gamma_l - 2(\gamma_s^d \gamma_l^d)^{1/2} - 2(\gamma_s^p \gamma_l^p)^{1/2} \tag{2}$$

By substituting equation (2) into Young's equation (1), the equation (1) becomes:

$$(1 + \cos \theta) \gamma_l = 2(\gamma_s^d \gamma_l^d)^{1/2} + 2(\gamma_s^p \gamma_l^p)^{1/2} \tag{3}$$

## 3. RESULTS

### 3.1. Physio-chemical characteristics of fiber.

All natural fibers primarily contain cellulose, hemicellulose, lignin and extractives. Table 2 shows the chemical composition of the presently fabricated fibers. This study found that the cellulose, lignin, holocellulose, hemicellulose, and extractives contents present in the fibers were 66.47, 2.39, 75.43, 9.43, and 2.11%,

respectively. In general, it was obvious that the cellulose content was higher compared to other compositions. It was well known that the chemical composition of natural fibers highly depends on several parameters such as the plant origin and growth conditions as reported in scientific literature. For instance, an analysis of the chemical composition of the raw flax fibers exhibited that the

moisture content, extractives, lignin, hemicellulose, and cellulose were 9.2, 6.2, 3.9, 15.7, and 64.8%, respectively [22].

Table 2. Chemical composition of the kenaf fiber

| Chemical composition | Percentage (%) |
|----------------------|----------------|
| Cellulose            | 66.47          |
| Lignin               | 2.39           |
| Holocellulose        | 75.43          |
| Hemicellulose        | 9.43           |
| Extractives          | 2.11           |

In addition, the density of the fiber is presented in Table 3. It was estimated that the fiber density was 1.00 g/cm<sup>3</sup>. It was reported from the previous study that the density of natural fibers ranged from 0.9 to 1.5 g/cm<sup>3</sup>. For instance, the extracted Alfa fibers have a density of 1.40 g/cm<sup>3</sup> [23]. In addition, the oil palm empty fruit bunch fibre has a density of 0.94 g/cm<sup>3</sup>. In general, it has been reviewed that the density of various natural fibers such as flax, hemp, jute, and harakeke are 1.5, 1.5, 1.3-1.5, and 1.3, respectively [24]. Moreover, it was also found that the length and diameter of the presently produced fibers were 897.07 μm and 66.38 μm, respectively, falling under microfiber category.

3.2. Biocomposites density.

Table 3 presents density of the presently produced biocomposites. Density of the biocomposite produced by mixing virgin ABS with 10% of filler was 1.067 g/cm<sup>3</sup>. A slight increase in the density for the biocomposite produced by mixing virgin ABS with 15%, which is 1.098 g/cm<sup>3</sup>. Alternatively, the biocomposite density fabricated by mixing recycled ABS with 10% of filler was 0.948 g/cm<sup>3</sup>. Also, a slight increase in the density for the biocomposite density fabricated by mixing recycled ABS with 15% of filler was 0.986 g/cm<sup>3</sup>.

Table 3. Density of the kenaf fiber and biocomposites

| Sample       | Density (g/cm <sup>3</sup> ) |
|--------------|------------------------------|
| Kenaf fiber  | 1.00                         |
| vABS-KSF-10% | 1.06                         |
| vABS-KSF-15% | 1.09                         |
| rABS-KSF-10% | 0.94                         |
| rABS-KSF-15% | 0.98                         |

3.3. Melt flow index of biocomposites.

Table 4 presents the melt flow index of the produced biocomposites. It was found that the melt flow index of the biocomposite produced by mixing with virgin ABS with 10% of filler was 6.5 g/10 min. An increase in the melt flow index of the biocomposite produced by mixing with virgin ABS with 15% was observed by 9.5 g/10 min.

Table 4. Melt flow index of the biocomposites

| Sample       | Melt Flow Index (g/10 min) |
|--------------|----------------------------|
| vABS-KSF-10% | 6.50                       |
| vABS-KSF-15% | 9.50                       |
| rABS-KSF-10% | 11.00                      |
| rABS-KSF-15% | 19.50                      |

A similar finding was also obtained for the biocomposite produced by mixing with recycled ABS. Enhancement of the value from 11.0 to 19.5 g/10 min can be obtained by increasing the filler contents from 10 to 15%. In general, the melt flow index of all produced biocomposites increased with increasing filler contents.

The melt flow index for recycled ABS was generally higher compared to virgin ABS.

An increase in the melt flow index of the biocomposites would help their injection moldability. It is possible to allow the addition of greater amounts of the natural fillers when compared to virgin ABS. Moreover, it was reported that the melt flow index characteristics of natural fibers are also influenced by their cellulose contents [25].

3.4. Surface free energy analysis.

Surface free energy is one of thermodynamic quantities that describes equilibrium state of atoms in surface layer of material. It is a combination of polar and nonpolar (dispersive) energy [26]. Surface free energy of the presently fabricated was estimated using the contact angle value. Surface free energy estimation of the biocomposites is presented in Table 5.

Table 5. Contact angle, dispersive component, polar component, and surface free energy of the biocomposites

| Sample       | Contact angle |        | Dispersive component | Polar component | Surface free energy |
|--------------|---------------|--------|----------------------|-----------------|---------------------|
|              | Water         | Hexane |                      |                 |                     |
| vABS-KSF-10% | 80.71         | 14.04  | 17.85                | 10.73           | 28.58               |
| vABS-KSF-15% | 94.85         | 16.28  | 17.67                | 4.03            | 21.70               |
| rABS-KSF-10% | 69.47         | 15.10  | 17.77                | 18.20           | 35.97               |
| rABS-KSF-15% | 68.92         | 17.55  | 17.55                | 18.75           | 36.30               |

Table 5 shows that the contact angle values of the biocomposites fabricated from the virgin ABS tested by the water increase with the rise of the filler contents of 10 and 15% by 80.71 and 94.85°, respectively. A similar finding was also observed for the biocomposites when tested using hexane by increasing from 14.04 and 16.28° for the filler contents of 10 and 15%, respectively. A slight difference of the contact angle characteristics was observed when the biocomposites were produced from the recycled ABS. It was found that the contact angle tested using the water was insignificantly decreased from 69.47 and 68.92° for the filler contents of 10 and 15%, respectively. Increasing the contact angle value indicates an increase in the hydrophobic nature of the biocomposites. It can also be suggested that enhancement of the contact angle values are related to the increase in surface roughness of the biocomposites.

Figures 1 and 2 illustrated the liquid droplet test for the produced biocomposites using the water and hexane for polar and dispersive components investigations, respectively. It was found that the polar component of the biocomposites produced from virgin ABS was decreased by 10.73 and 4.03 for the filler contents of 10 and 15%, respectively. A decrease in the dispersive component was also observed for the biocomposites by 17.85 and 17.67 for the corresponding filler contents. In addition, the polar component of the biocomposites produced from recycled ABS were 18.20 and 18.75 for the filler contents of 10 and 15%, respectively. Moreover, the dispersive component of the biocomposites for the corresponding filler contents was 17.77 and 17.55.

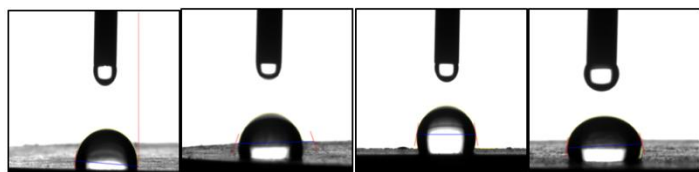


Figure 1. Polar component test for the produced biocomposites

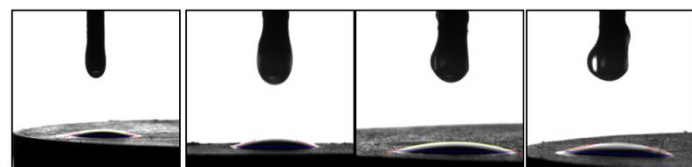


Figure 2. Dispersive component test for the produced biocomposites

In general, the surface free energy of the biocomposites produced from virgin ABS was decreased by 28.58 and 21.70 for the filler contents of 10 and 15%, respectively. Alternatively, the surface free energy of the biocomposites produced from recycled ABS was slightly increased by 35.97 and 36.30 for the corresponding filler contents. The polar component of the biocomposites was responsible for increasing their surface energy.

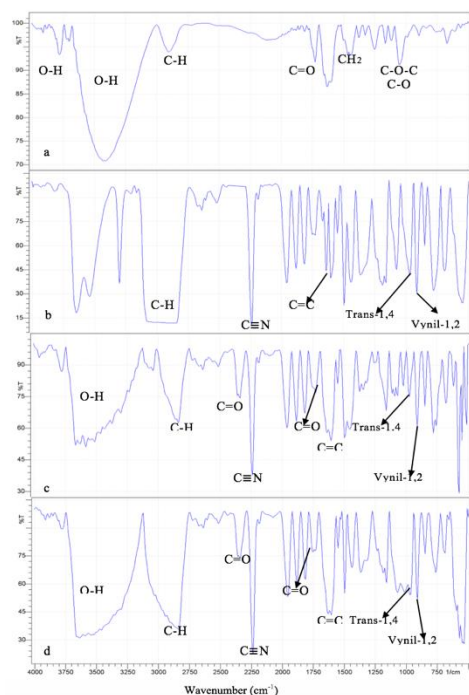


Figure 3. FTIR spectra of (a) kenaf fibers, (b) virgin ABS, (c) vABS-KSF-10%, and (d) vABS-KSF-15%.

### 3.5. FTIR inspection.

FTIR analysis was conducted to determine the changes in functional groups of the biocomposites. Atomic and molecular compositions of the fibers and matrix surface are different. When the surface of fibers and the matrix bonds, it forms a specific chemical bond. The atoms in molecule vibrate to describe the vibrational energy levels. If the molecule absorbs infrared radiation, it would be excited to its higher level. Cellulose molecules have a strong tendency to form hydrogen bonds intra- and intermolecularly.

FTIR spectra are shown in Figures 3 and 4 show several peaks, which are at 3410  $\text{cm}^{-1}$ , 2901  $\text{cm}^{-1}$ , 1443  $\text{cm}^{-1}$ , and 1057  $\text{cm}^{-1}$  due to hydrogen bonding (OH), C-H, CH<sub>2</sub>, and C-O-C or C-O stretching. In addition, Figures 3 and 4 present the infrared absorption for the virgin and recycled ABS, respectively. Acrylonitrile monomer peak was identified to exist at the

wavenumber of 2237  $\text{cm}^{-1}$ . In addition, aromatic ring for styrene was found at wavenumber 1643  $\text{cm}^{-1}$  and the double bond of butadiene and vnyl was observed at 964  $\text{cm}^{-1}$  and 910  $\text{cm}^{-1}$ , respectively [27].

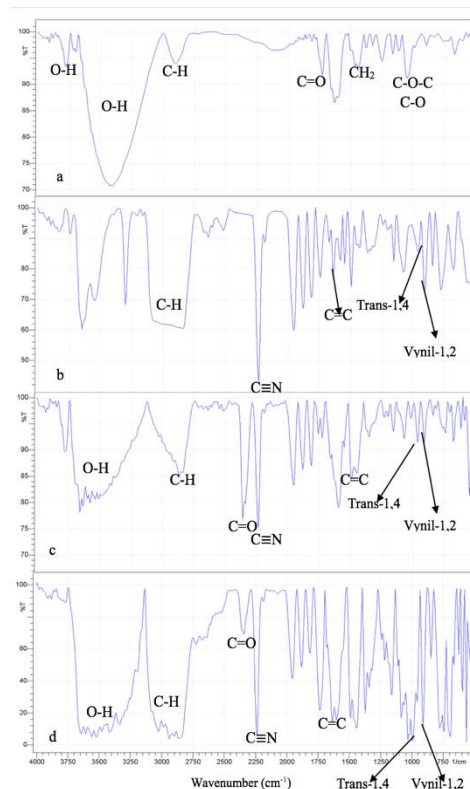


Figure 4. FTIR spectra of (a) kenaf fibers, (b) recycled ABS, (c) rABS-KSF-10%, and (d) rABS-KSF-15%.

FTIR spectra for the biocomposites were dominated by peaks of the ABS polymer. There were no significant transmittance changes at acrylonitrile monomer peak. Aromatic ring for styrene experiences the change of transmittance with the increase in the filler content in the biocomposites. The change for OH peak transmittance in the biocomposites indicated a reaction between the hydroxyl groups of filler binding with the carboxyl hydroxyl groups of maleic anhydride [28]. Maleic anhydride was successfully grafted on butadiene chain.

Based on the FTIR spectra, intensity of butadiene in the biocomposites was changed when it is compared with ABS polymer because the double bond of butadiene (C<sub>4</sub> and C<sub>5</sub>) binded C<sub>2</sub> and C<sub>3</sub> from maleic anhydride by covalent bonding. Figure 3 also shows changes in the transmittance intensity for trans and vnyl, which are increased with increasing filler contents in the biocomposites. The wavenumber of ester carbonyl (C=O) was observed at 1728  $\text{cm}^{-1}$ , 1751  $\text{cm}^{-1}$ , 1790  $\text{cm}^{-1}$ , and 1736  $\text{cm}^{-1}$  for vABS-KSF-10%, vABS-KSF-15%, rABS-KSF-10%, and rABS-KSF-15%, respectively. This ester carbonyl promotes the binding between the kenaf fibers with maleic acid by esterification. Esterification of cellulose with carboxylic derivatives occurs through a mechanism of derivatives cyclic carboxylic acid due to heating treatment at a temperature of 170 °C [29].

Analysis of the functional groups on the biocomposites showed the shifting and changing of the functional groups that are influenced by their treatment procedure. These shifting and changing of the functional groups for the biocomposites also demonstrated variation in the chemical bonding which is possibly

due to the changes of tissue structure of the polymer matrix. In general, findings from this study contribute significantly on the development of materials derived from natural resources. Although synthetic materials are also promising for certain applications [30-

#### 4. CONCLUSION

The present study has discussed the fabrication and evaluation of the physio-chemical features of composites filled with natural resources. It was interesting to note that the addition of short kenaf fibers for fabricating biocomposites affected their density and the melt flow index. Surface free energy of the biocomposites fabricated using virgin ABS was demonstrated to decrease with

#### 5. REFERENCES

- Gutiérrez, T.J.; Alvarez, V.A. Bionanocomposite films developed from corn starch and natural and modified nano-clays with or without added blueberry extract. *Food Hydrocolloids* **2018**, *77*, 407-420, <https://doi.org/10.1016/j.foodhyd.2017.10.017>.
- Aich, P.; An, J.; Yang, B.; Ko, Y.H.; Kim, J.; Murray, J.; Cha, H.J.; Roh, J.H.; Park, K.M.; Kim, K. Self-assembled adhesive biomaterials formed by a genetically designed fusion protein. *Chemical Communications* **2018**, *54*, 12642-12645, <https://doi.org/10.1039/C8CC07475E>.
- Ruskowitz, E.R.; DeForest, C.A. Photoresponsive biomaterials for targeted drug delivery and 4D cell culture. *Nature Reviews Materials* **2018**, *3*, 17087, <https://doi.org/10.1038/natrevmats.2017.87>.
- Balta, S.; Aydogan, C.; Demir, B.; Geyik, C.; Ciftci, M.; Guler, E.; Odaci Demirkol, D.; Timur, S.; Yagci, Y. Functional surfaces constructed with hyperbranched copolymers as optical imaging and electrochemical cell sensing platforms. *Macromolecular Chemistry and Physics* **2018**, *219*, 1-10, <https://doi.org/10.1002/macp.201700433>.
- Wen, J.; Yeh, C.-K.; Sun, Y. Salivary polypeptide/hyaluronic acid multilayer coatings act as "fungal repellents" and prevent biofilm formation on biomaterials. *Journal of Materials Chemistry B* **2018**, *6*, 1452-1457, <https://doi.org/10.1039/C7TB02592K>.
- Rilda, Y.; Safitri, R.; Agustien, A.; Nazir, N.; Syafiuddin, A.; Nur, H. Enhancement of antibacterial capability of cotton textiles coated with TiO<sub>2</sub>-SiO<sub>2</sub>/Chitosan using hydrophobization. *Journal of the Chinese Chemical Society* **2017**, *64*, 1347-1353, <https://doi.org/10.1002/jccs.201700165>.
- Nikmatin, S.; Syafiuddin, A.; Irwanto, D.A.Y. Properties of oil palm empty fruit bunch-filled recycled acrylonitrile butadiene styrene composites: Effect of shapes and filler loadings with random orientation. *BioResources* **2016**, *12*, 1090-1101, <https://doi.org/10.15376/biores.12.1.1090-1101>.
- Nikmatin, S.; Syafiuddin, A.; Hong Kueh, A.B.; Maddu, A. Physical, thermal, and mechanical properties of polypropylene composites filled with rattan nanoparticles. *Journal of Applied Research and Technology* **2017**, *15*, 386-395, <https://doi.org/10.1016/j.jart.2017.03.008>.
- Nikmatin, S.; Hermawan, B.; Irmansyah, I.; Indro, M.N.; Kueh, A.B.H.; Syafiuddin, A. Evaluation of the performance of helmet prototypes fabricated from acrylonitrile butadiene styrene composites filled with natural resource. *Materials* **2019**, *12*, 1-12, <https://doi.org/10.3390/ma12010034>.
- Nikmatin, S.; Syafiuddin, A.; Kueh, A.B.H.; Purwanto, Y.A. Effects of nanoparticle filler on thermo-physical properties of rattan powder-filled polypropylene composites. *Jurnal Teknologi* **2015**, *77*, 181-187, <https://doi.org/10.11113/jt.v77.6415>.
- Feng, X.; Yang, Z.; Rostom, S.S.; Dadmun, M.; Wang, S.; Wang, Q.; Xie, Y. Reinforcing 3D printed acrylonitrile butadiene styrene by impregnation of methacrylate resin and cellulose nanocrystal mixture: Structural effects and homogeneous properties. *Materials & Design* **2018**, *138*, 62-70, <https://doi.org/10.1016/j.matdes.2017.10.050>.
- Ku, H.; Wang, H.; Pattarachaiyakoo, N.; Trada, M. A review on the tensile properties of natural fiber reinforced polymer composites. *Composites Part B: Engineering* **2011**, *42*, 856-873, <https://doi.org/10.1016/j.compositesb.2011.01.010>.
- John, M.J.; Thomas, S. Biofibres and biocomposites. *Carbohydrate Polymers* **2008**, *71*, 343-364, <https://doi.org/10.1016/j.carbpol.2007.05.040>.
- Sarikaya, E.; Çallioğlu, H.; Demirel, H. Production of epoxy composites reinforced by different natural fibers and their mechanical properties. *Composites Part B: Engineering* **2019**, *167*, 461-466, <https://doi.org/10.1016/j.compositesb.2019.03.020>.
- Mishra, R.; Wiener, J.; Militky, J.; Petru, M.; Tomkova, B.; Novotna, J. Bio-composites reinforced with natural fibers: comparative analysis of thermal, static and dynamic-mechanical properties. *Fibers and Polymers* **2020**, *21*, 619-627, <https://doi.org/10.1007/s12221-020-9804-0>.
- Sumesh, K.R.; Kanthavel, K.; Kavimani, V. Peanut oil cake-derived cellulose fiber: Extraction, application of mechanical and thermal properties in pineapple/flax natural fiber composites. *International Journal of Biological Macromolecules* **2020**, *150*, 775-785, <https://doi.org/10.1016/j.ijbiomac.2020.02.118>.
- Topcu, C.; Caglar, B.; Onder, A.; Coldur, F.; Caglar, S.; Guner, E.K.; Cubuk, O.; Tabak, A. Structural characterization of chitosan-smectite nanocomposite and its application in the development of a novel potentiometric monohydrogen phosphate-selective sensor. *Materials Research Bulletin* **2018**, *98*, 288-299, <https://doi.org/10.1016/j.materresbull.2017.09.068>.
- Rathinam, K.; Singh, S.P.; Arnusch, C.J.; Kasher, R. An environmentally-friendly chitosan-lysozyme biocomposite for the effective removal of dyes and heavy metals from aqueous solutions. *Carbohydrate Polymers* **2018**, *199*, 506-515, <https://doi.org/10.1016/j.carbpol.2018.07.055>.
- Li, X.; Yang, Y.; Fan, Y.; Feng, Q.; Cui, F.Z.; Watari, F. Biocomposites reinforced by fibers or tubes as scaffolds for tissue engineering or regenerative medicine. *Journal of Biomedical Materials Research Part A* **2014**, *102*, 1580-1594, <https://doi.org/10.1002/jbm.a.34801>.
- Young, T. An essay on the cohesion of fluids. *Philosophical Transactions of the Royal Society of London* **1805**, *95*, 65-87, <https://doi.org/10.1098/rstl.1805.0005>.
- Owens, D.K.; Wendt, R. Estimation of the surface free energy of polymers. *Journal of Applied Polymer Science* **1969**, *13*, 1741-1747, <https://doi.org/10.1002/app.1969.070130815>.

34], the use of natural resources can be valuable not only on the designing new alternative materials but also for the environmental management practices via reducing wastes [35-37].

increasing filler content. However, it was found that their characteristic of biocomposites fabricated using recycled ABS was slightly improved. In addition, FTIR observation exhibited that the addition of the natural fibers in the virgin and recycled ABS performed a slightly different characteristic.

22. Astruc, J.; Nagalakshmaiah, M.; Laroche, G.; Grandbois, M.; Elkoun, S.; Robert, M. Isolation of cellulose-II nanospheres from flax stems and their physical and morphological properties. *Carbohydrate Polymers* **2017**, *178*, 352-359, <https://doi.org/10.1016/j.carbpol.2017.08.138>.
23. Brahim, S.B.; Cheikh, R.B. Influence of fibre orientation and volume fraction on the tensile properties of unidirectional Alfa-polyester composite. *Composites Science and Technology* **2007**, *67*, 140-147, <https://doi.org/10.1016/j.compscitech.2005.10.006>.
24. Pickering, K.L.; Efendy, M.G.A.; Le, T.M. A review of recent developments in natural fibre composites and their mechanical performance. *Composites Part A: Applied Science and Manufacturing* **2016**, *83*, 98-112, <https://doi.org/10.1016/j.compositesa.2015.08.038>.
25. Chevali, V.S.; Nerenz, B.A.; Ulven, C.A.; Kandare, E. Mechanical properties of hybrid lignocellulosic fiber-filled acrylonitrile butadiene styrene (ABS) biocomposites. *Polymer-Plastics Technology and Engineering* **2015**, *54*, 375-382, <https://doi.org/10.1080/03602559.2014.961078>.
26. Rudawska, A.; Jacniacka, E. Analysis for determining surface free energy uncertainty by the Owen-Wendt method. *International Journal of Adhesion and Adhesives* **2009**, *29*, 451-457, <https://doi.org/10.1016/j.ijadhadh.2008.09.008>.
27. Polli, H.; Pontes, L.; Araujo, A.; Barros, J.M.; Fernandes, V. Degradation behavior and kinetic study of ABS polymer. *Journal of Thermal Analysis and Calorimetry* **2009**, *95*, 131-134, <https://doi.org/10.1007/s10973-006-7781-1>.
28. Ma, H.; Xu, Z.; Tong, L.; Gu, A.; Fang, Z. Studies of ABS-graft-maleic anhydride/clay nanocomposites: Morphologies, thermal stability and flammability properties. *Polymer Degradation and Stability* **2006**, *91*, 2951-2959, <https://doi.org/10.1016/j.polyimdegradstab.2006.08.017>.
29. Yang, H.S.; Wolcott, M.; Kim, H.S.; Kim, H.J. Thermal properties of lignocellulosic filler-thermoplastic polymer biocomposites. *Journal of Thermal Analysis and Calorimetry* **2005**, *82*, 157-160, <https://doi.org/10.1007/s10973-005-0857-5>.
30. Syafiuddin, A.; Salmiati, S.; Hadibarata, T.; Salim, M.R.; Kueh, A.B.H.; Sari, A.A., A purely green synthesis of silver nanoparticles using *Carica papaya*, *Manihot esculenta*, and *Morinda citrifolia*: Synthesis and antibacterial evaluations. *Bioprocess and Biosystems Engineering*, **2017**, *40*, 1349-1361, <https://doi.org/10.1007/s00449-017-1793-z>.
31. Syafiuddin, A.; Salmiati, S.; Salim, M.R.; Kueh, A.B.H.; Hadibarata, T.; Nur, H., A review of silver nanoparticles: Research trends, global consumption, synthesis, properties, and future challenges. *Journal of the Chinese Chemical Society*, **2017**, *64*, 732-756, <https://doi.org/10.1002/jccs.201700067>.
32. Syafiuddin, A.; Hadibarata, T.; Zon, N.F.; Salmiati, Characterization of titanium dioxide doped with nitrogen and sulfur and its photocatalytic appraisal for degradation of phenol and methylene blue. *Journal of the Chinese Chemical Society*, **2017**, *64*, 1333-1339, <https://doi.org/10.1002/jccs.201700136>.
33. Syafiuddin, A., Toward a comprehensive understanding of textiles functionalized with silver nanoparticles. *Journal of the Chinese Chemical Society*, **2019**, *66*, 793-814, <https://doi.org/10.1002/jccs.201800474>.
34. Syafiuddin, A.; Salmiati, S.; Hadibarata, T.; Kueh, A.B.H.; Salim, M.R., Novel weed-extracted silver nanoparticles and their antibacterial appraisal against a rare bacterium from river and sewage treatment plan. *Nanomaterials*, **2018**, *8*, 1-17, <https://doi.org/10.3390/nano8010009>.
35. Syafiuddin, A.; Fulazzaky, M.A.; Salmiati, S.; Kueh, A.B.H.; Fulazzaky, M.; Salim, M.R., Silver nanoparticles adsorption by the synthetic and natural adsorbent materials: an exclusive review. *Nanotechnology for Environmental Engineering*, **2020**, *5*, 1-18, <https://doi.org/10.1007/s41204-019-0065-3>.
36. Syafiuddin, A.; Salmiati, S.; Hadibarata, T.; Kueh, A.B.H.; Salim, M.R.; Zaini, M.A.A., Silver nanoparticles in the water environment in Malaysia: Inspection, characterization, removal, modeling, and future perspective. *Scientific Reports*, **2018**, *8*, 1-15, <https://doi.org/10.1038/s41598-018-19375-1>.
37. Syafiuddin, A.; Salmiati, S.; Hadibarata, T.; Salim, M.R.; Kueh, A.B.H.; Suhartono, S., Removal of silver nanoparticles from water environment: Experimental, mathematical formulation, and cost analysis. *Water, Air, and Soil Pollution*, **2019**, *230*, 102-117, <https://doi.org/10.1007/s11270-019-4143-8>.

## 6. ACKNOWLEDGEMENTS

The present study was fully funded by the BPPTN research of strategic application under contract no. 079/SP2H/LT/DRPM/II/2016 from the Directorate General of Strengthening Research and Development, Ministry of Research, Technology and Higher Education, Republic of Indonesia. The authors also thank the IPB University for facilitating the study.



© 2020 by the authors. This article is an open access article distributed under the terms and conditions of the Creative Commons Attribution (CC BY) license (<http://creativecommons.org/licenses/by/4.0/>).